



Measuring the drying rate of liquid film coatings using heat-flux method

著者	Yamamura Masato, Ohara Keiji, Mawatari Yoshihide, Kage Hiroyuki
journal or publication title	Drying Technology
volume	27
number	6
page range	817-820
year	2009-06-04
URL	http://hdl.handle.net/10228/00006353

doi: info:doi/10.1080/07373930902901687

Measuring the drying rate of liquid film coatings using heat-flux method

Masato Yamamura, Keiji Ohara, Yoshihide Mawatari, Hiroyuki Kage

Department of Applied Chemistry, Kyushu Institute of Technology,

Sensui 1-1, Tobata, Kitakyushu, Fukuoka 804-8550 Japan

TEL: 093-884-3344, FAX: 093-884-3300, yamamura@che.kyutech.ac.jp

ABSTRACT

We propose a simple method of determining solvent-drying rates from heat-flux measurements across thin liquid films. The theory is based on quasi-steady conductive heat transport through coatings, combined with simultaneous heat and mass transfers in the gas phase. The measured evaporation rates well reproduce conventional gravimetric measurements with an uncertainty of less than 5 %. Drying experiments also revealed that the proposed method is robust in systems with high levels of fluctuation and thus provide an alternative tool for monitoring drying kinetics in forced airflows.

1. INTRODUCTION

To produce thin film coatings, a liquid on a substrate is dried in an unsaturated gas phase or under a forced airflow condition. Understanding removal rates of the solvent from a gas-liquid interface is of practical and fundamental importance. The conventional gravimetric method [1-3], by which a coating weight loss per unit area is measured over time, is often disturbed by fluctuations of the flowing air and is thus limited to low drying rates. Although recent progress in infrared- [4,5] and confocal-Raman- [6] spectroscopies has enabled us to quantify local solvent concentrations in evaporating multi-component liquids, careful calibrations are usually required for each chemical species. Furthermore, the need for optical transparency at the wavelength of interest often limits the applicability of these techniques to samples ~10 microns thick or less. Direct measurements of solvent gas compositions [7] provide an alternative method of determining the drying rate of thick, opaque films in high-speed airflows, but are currently limited to homogeneously drying samples because compositional variations in the “well-mixed” gas phase only give spatially averaged evaporation rates along the coating surface.

In this article, we report a novel method based on a local heat-flux measurement to determine solvent-drying rates without a need for sample transparency. The similar

measurement technique has been previously proposed for wood drying [8], but it required an empirical correction factor to fit weight loss measurements and has been limited to materials with axi-symmetric temperature profiles. The present study deals with more general cases by considering rigorous heat transfer models. In Section 2, we derive the quasi-steady heat balance equation that directly links the solvent-drying rate with the heat flux through the coating. Section 3 describes the experimental setup of the heat-flux measurement combined with the gravimetric technique. The proposed theory is verified in Section 4 from the simultaneous mass/heat-flux measurements for thin solvent liquid layers. Conclusions are presented in Section 5.

2. THEORY

Consider an evaporating liquid film coated on an impermeable substrate (Fig. 1). The upper gas-liquid interface is exposed to a gas phase unsaturated with solvent vapor. Assuming a negligible gas thermal capacity, the total heat flux in the gas phase, q^G , is a sum of the latent heat flux via the solvent evaporation and the convective heat flux driven by the temperature difference between the bulk and the interface as:

$$q^G = r(t)\Delta H + h_{\text{sol}}^G(T_i - T_b). \quad (1)$$

where $r(t)$ denotes the time-dependent drying rate of the solvent, ΔH is the latent heat, h_{sol}^G is the heat-transfer coefficient on the evaporating interface, T_i is the gas/liquid

interface temperature, and T_b is the temperature in bulk gas.

The temperature profile in the coating becomes linear when the heat-transfer resistance in the coating is sufficiently small compared to that in the gas phase. Based on a quasi-steady-state approximation, the conductive heat fluxes in the liquid layer of thickness h and in the substrate of thickness H are respectively expressed as:

$$q^L = \lambda \frac{T_{fb} - T_i}{h}, \quad (3)$$

$$q^S = \lambda_s \frac{T_s - T_{fb}}{H}. \quad (4)$$

where λ and λ_s denote the thermal conductivities in the liquid and the substrate, respectively. T_{fb} and T_s are the temperatures at the liquid-solid interface and the lower substrate surface.

The heat balances at the air-liquid and liquid-solid interfaces $q^G = q^L = q^S$ yield the expressions for the surface temperature and the solvent-drying rate as:

$$T_i = T_s - \frac{\left(\frac{\lambda}{h}\right) + \left(\frac{\lambda_s}{H}\right)}{\left(\frac{\lambda}{h}\right)\left(\frac{\lambda_s}{H}\right)} q^S. \quad (5)$$

$$r(t) = \frac{1}{\Delta H} \left\{ q^S + h_{sol}^G \frac{\left(\frac{\lambda}{h}\right) + \left(\frac{\lambda_s}{H}\right)}{\left(\frac{\lambda}{h}\right)\left(\frac{\lambda_s}{H}\right)} q^S - h_{sol}^G (T_s - T_b) \right\}. \quad (6)$$

The second term on the right-hand side of Eqs. (5)-(6) can be deduced when the heat-transfer resistances in the liquid and the substrate are sufficiently small. The last

term in Eq. (6) denotes the contribution of the sensible heat flux in the gas phase.

The heat flux before liquid deposition can be given in a simpler form as:

$$q_0^S = h_{\text{air}}^G (T_{s0} - T_b). \quad (7)$$

where h_{air}^G denotes the heat-transfer coefficient on the solid substrate in air, and T_{s0} is the initial surface temperature of the substrate. Combining Eqs. (6)-(7) gives the expression for the drying rate as:

$$r(t) = \frac{1}{\Delta H} \left[\left[1 + \alpha \frac{(\lambda/h)^+ (\lambda_s/H)}{(\lambda/h) (\lambda_s/H)} \frac{q_0^S}{T_{s0} - T_b} \right] q^S(t) - \alpha \left(\frac{T_s(t) - T_b}{T_{s0} - T_b} \right) q_0^S \right]. \quad (8)$$

where $\alpha \equiv h_{\text{sol}}^G / h_{\text{air}}^G$ is the ratio of heat-transfer coefficients in the solvent vapor to the air. Thus simultaneous measurements of the total heat flux, $q^S(t)$, and the substrate bottom temperature, $T_s(t)$, allow us to determine the solvent-drying rate from Eq. (8) as a function of the elapsed drying time. In the following section we represent drying experiments to verify the theory.

3. EXPERIMENTAL APPARATUS AND PROCEDURE

The drying apparatus is shown schematically in Fig. 2. The sample liquid was ethanol used as purchased with no further purification. The sample physical properties are summarized in Table 1. The test liquid was coated on a 1-mm thick clean glass substrate with an initial film thickness of 500 μm . The coated area was specified to be 9 cm^2 by

gluing 1.0-mm thick aluminum shims on the substrate. The substrate was continuously heated by a glass conductive heater (MP-10DMH, Kitazato) set beneath the substrate with an air clearance of 1.5 mm. The substrate temperature was maintained at a constant value ranging between 308.2 K and 333.2 K by regulating the current through the heater. A heat-flux sensor (HF, Captech) was glued beneath the substrate using a conductive grease in order to measure the heat flux $q^S(t)$. The sensor consisted of thermocouple arrays and gave a voltage proportional to the conductive heat flux with a sensitivity of 307 (W/m²)/mV. The voltage measurement error was estimated to be $\pm 6 \mu\text{V}$, which corresponds to the uncertainty of measured heat flux of $\pm 2 \text{ W/ m}^2$. The characteristic response time of the sensor was 100 ms, which was sufficiently short compared to the drying time scale of interest.

The coating was then mounted on an electronic balance (CP423S, Sartorius) in order to perform simultaneous measurements of the heat flux and the sample weight-loss. The measured heat flux, the substrate bottom temperature, and the coating mass were stored in a personal computer at a sampling rate of 0.2 Hz. The solvent-drying rate from the gravimetry was calculated from each slope of the weight-loss curves as $r = - (1/A)dW/dt$, where A is the film surface area, t is the time, and W is the mass of the film during drying. An average of 40 neighboring data points was taken as a smoothed W

value at each time and used in the calculations.

4. RESULTS AND DISCUSSION

Variations in the measured heat flux and the substrate bottom temperature can be divided into four distinct regimes, as shown in Fig. 3. Before the liquid deposition (Regime I), the test fluid was pre-heated to the initial substrate temperature, and the measured flux shows a non-zero constant value q_0^S , which is attributed to the sensible heat flux in air in Eq. (7). The subsequent coating operation resulted in a rapid decrease in substrate temperature and an increase in the heat flux (Regime II). The measured flux tends to maintain a constant value in the intermediate Regime III, then drops at a certain drying time t_d , and eventually converges into the initial value q_0^S (Regime IV). The preliminary coating visualization reveals that the liquid film spontaneously ruptures at t_d to leave a non-wetted area on the substrate surface, implying that the decrease in the measured heat flux results from a reduction of the effective evaporation area due to film de-wetting. This result is also consistent with the rapid increase in the substrate temperature in Regime IV.

The boundary layer theory [9] shows that the convective heat-transfer coefficients in most simple flow fields are proportional to $Pr^{1/3}$, where the Prandtl number is defined with respect to the fluid viscosity μ , the thermal capacity C_p , and the thermal

conductivity λ as $Pr \equiv \mu C_p / \lambda$. The theory allows one to use Eq. (8) to estimate the ratio of heat-transfer coefficients in the solvent vapor to the air, $\alpha \equiv h_{\text{sol}}^G / h_{\text{air}}^G$, as :

$$\alpha = \frac{\lambda_{\text{sol}}}{\lambda_{\text{air}}} \left(\frac{Pr_{\text{sol}}}{Pr_{\text{air}}} \right)^{1/3}. \quad (9)$$

where the subscripts sol and air represent the evaporating solvent and the air, respectively. We calculated the solvent-drying rates using the measured heat flux and the substrate-temperature data, as well as the heat-transfer ratio from Eq. (9). Figure 4 depicts comparisons between the calculated drying rates from the heat-flux method and those from the simultaneous gravimetry for four different substrate temperatures of (a)308.2 K, (b)313.2 K, (c)318.2 K, and (d) 323.2 K, respectively . As expected, the evaporation at higher temperatures results in shorter times to complete drying. The heat-flux measurement is in good agreement with the weight-loss measurement in whole drying regimes. The gravimetric measurement was found to be disturbed by system fluctuations during the evaporation, whereas the heat-flux method gives a smoother drying rate curve under the same drying condition, suggesting that the heat-flux method is free from external fluctuations and thus applicable to practical drying conditions in forced airflows.

In order to verify the proposed method in detail, we calculated the time-averaged drying rate in Regime III (see Fig. 3) using heat-flux and gravimetric methods. As

shown in Fig. 5, the drying rates measured by the heat-flux method well reproduce those from the conventional gravimetric technique within a relative error of $\pm 5\%$, providing unambiguous evidence that the heat-flux method allows us to determine the solvent-drying rate in a quantitative sense.

It is worth noting that the heat-flux method does not require optical transparency of samples nor temperature uniformity across the coating. The former demonstrates a great advantage over previously reported spectroscopic techniques because the present method is potentially applicable to systems, in which the transmitted light signals may be reduced due to light scatters via solid-fillers and/or phase-separated domains involved in the film.

For a specific case when the temperature distribution across the coating can be neglected in whole drying regimes, Nishimura et al. [10] have recently proposed a novel drying rate measurement technique using time-dependent heat balance equations. However, their model requires the heat-transfer coefficient or the final residual solvent contents *a priori*. The present method directly determines the heat-transfer coefficient from the heat-flux measurement, and is thus applicable to practical drying conditions where steep temperature gradients can develop in evaporating films.

5. CONCLUSIONS

We propose a new method to determine solvent-drying rates based on a simple local heat-flux measurement. The present method is free from system fluctuations and does not require optical transparency of samples. A quasi-steady, heat/mass transfer model was derived to calculate the solvent-drying rate from simultaneous measurements of the heat flux and the substrate temperature. Drying experiments revealed that solvent-drying rates measured from the heat-flux method agree well with those from the conventional gravimetric method within a relative error of $\pm 5\%$, suggesting the validity of the proposed theory in a quantitative sense.

LITERATURE CITED

- 1) Foerst, P.; Kulozik, U. Validation of a novel in situ weighing system during vacuum drying. *Drying Technology* 2007, 25(5), 767-773.
- 2) Yamamura, M.; Nishio T.; Kajiwara, T.; Adachi, K. Effect of stepwise change of drying rate on microstructure evolution in polymer films. *Drying Technology* 2002, 20(7), 1393-1405.
- 3) Yamamura, M.; Orihashi, K.; Mawatari, Y.; Kage, H. Light-tunable solvent drying in photo-responsive solution coatings. *Drying Technology* 2008, 26(1), 97-100.
- 4) Saure, R.; Wagner, G.R.; Schlunder E.-U. Drying of solvent-borne polymeric coatings: II. Experimental results using FTIR spectroscopy. *Surface and Coatings Technology* 1998, 99, 257-265.
- 5) Suzuki, I.; Yasui, Y.; Udagawa, A.; Kawate, K. Drying process monitoring by rapid scanning FT-IR spectrometer. *Industrial Coating Research* 2004, 5, 107-123.
- 6) Ludwig, I.; Schabel, W.; Kind, M. Drying and Film Formation of Industrial Waterborne Latices. *AIChE Journal* 2007, 53(3), 549-560.
- 7) Vinjamur, M.; Cairncross, R.A. A high airflow drying experimental set-up to study drying behavior of polymer solvent coatings. *Drying Technology* 2001, 19(8), 1591-1612.

- 8) Vanek, M. Determination of the evaporation of water during wood drying by means of heat flux measurement. *Drying Technology* 1992, 10(5), 1207-1217.
- 9) Schlichting, H. 1968. *Boundary-layer Theory* (3th edition), 292, McGraw-Hill.
- 10) Nishimura, N.; Takigawa, T.; Iyota, H.; Imakoma, H. Measurement of drying rate from temperature data during drying of slab materials (in Japanese). *Kagaku Kogaku Ronbunshu* 2007, 33(2), 101-106.

LIST OF FIGURES

Table 1 Sample properties

Figure 1 Drying configurations

Figure 2 Experimental apparatus.

Figure 3 Variations in bottom temperature and heat flux for the initial bottom temperature of $T_{S0}=313.2$ K. The drying regime is subdivided into four Regimes as (I) before film deposition, (II) onset of evaporation, (III) quasi-state state before film dewetting, (IV) after the dewetting. The air temperature is $T_b=296.3$ K, and the heat transfer coefficient determined from Eq. (7) was found to be $h_{air}^G=9.8$ W/(m²K).

Figure 4 Comparisons between the heat flux (solid curves) and gravimetric (rectangular symbols) methods for four different substrate temperatures of (a)308.2 K, (b)313.2 K, (c)318.2 K and (d) 323.2 K.

Figure 5 Comparison of the time-averaged drying rates between the heat flux method and the gravimetric method. The measured drying rates agree within a relative error of $\pm 5\%$.

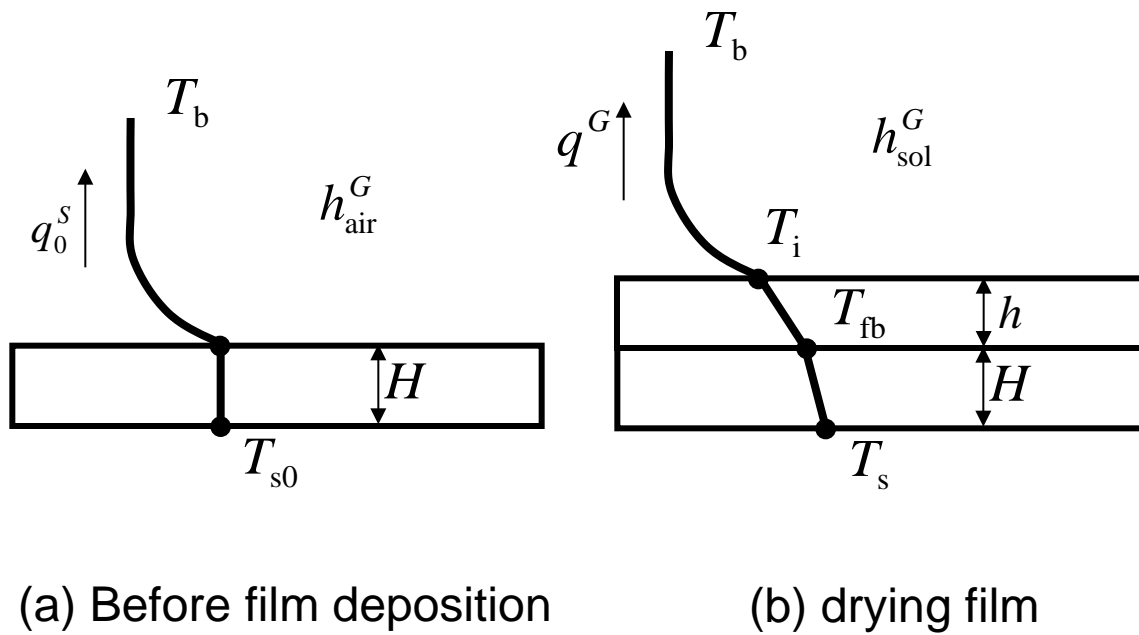


Fig. 1 Drying configurations

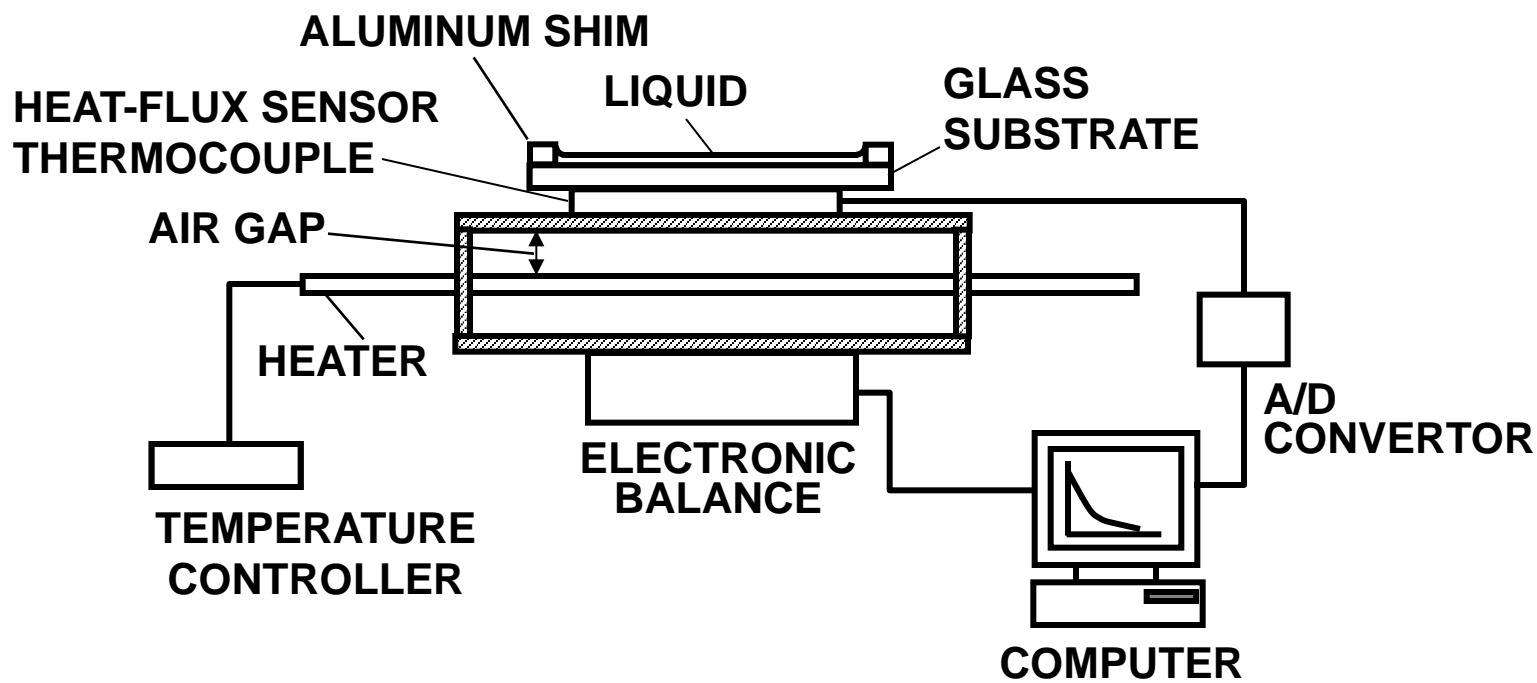


Fig.2 Experimental apparatus.

Table 1 Sample properties

Latent heat [kJ/kg]	837.9
thermal conductivity of ethanol (liquid) [W/(m·K)]	0.166
thermal conductivity of ethanol (gas) [mW/(m·K)]	14.5
heat capacity of ethanol (gas) [kJ/(kg·K)]	1.42
viscosity(gas) [$\mu\text{Pa}\cdot\text{s}$]	8.12
α [-]	0.573
thermal conductivity of substrate [W/(m·K)]	1.04
thickness of substrate [mm]	1.3

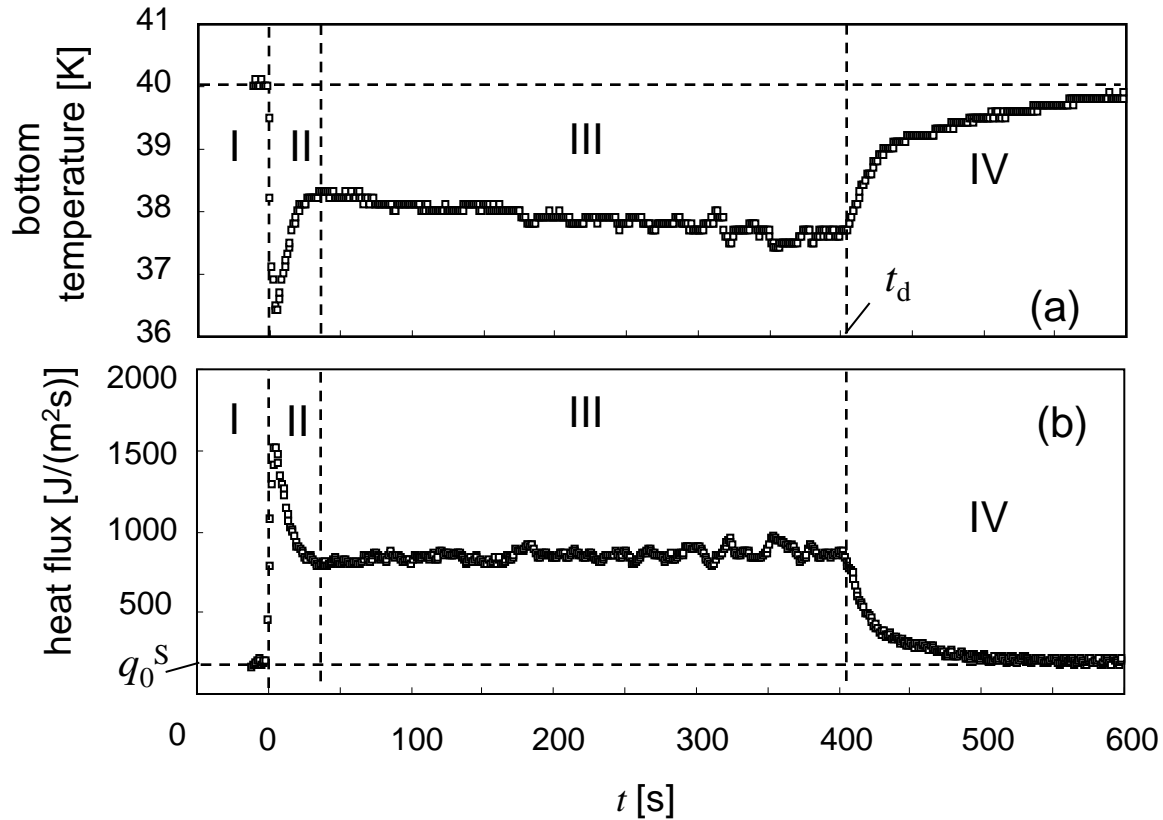


Fig.3 Variations in bottom temperature and heat flux for the initial bottom temperature of $T_{s0}=313.2$ K. The drying regime is subdivided into four Regimes as (I) before film deposition, (II) onset of evaporation, (III) quasi-state state before film dewetting, (IV) after the dewetting. The air temperature is $T_b=296.3$ K, and the heat transfer coefficient determined from Eq. (7) was found to be $h_{\text{air}}^G=9.8$ $\text{W}/(\text{m}^2\text{K})$.

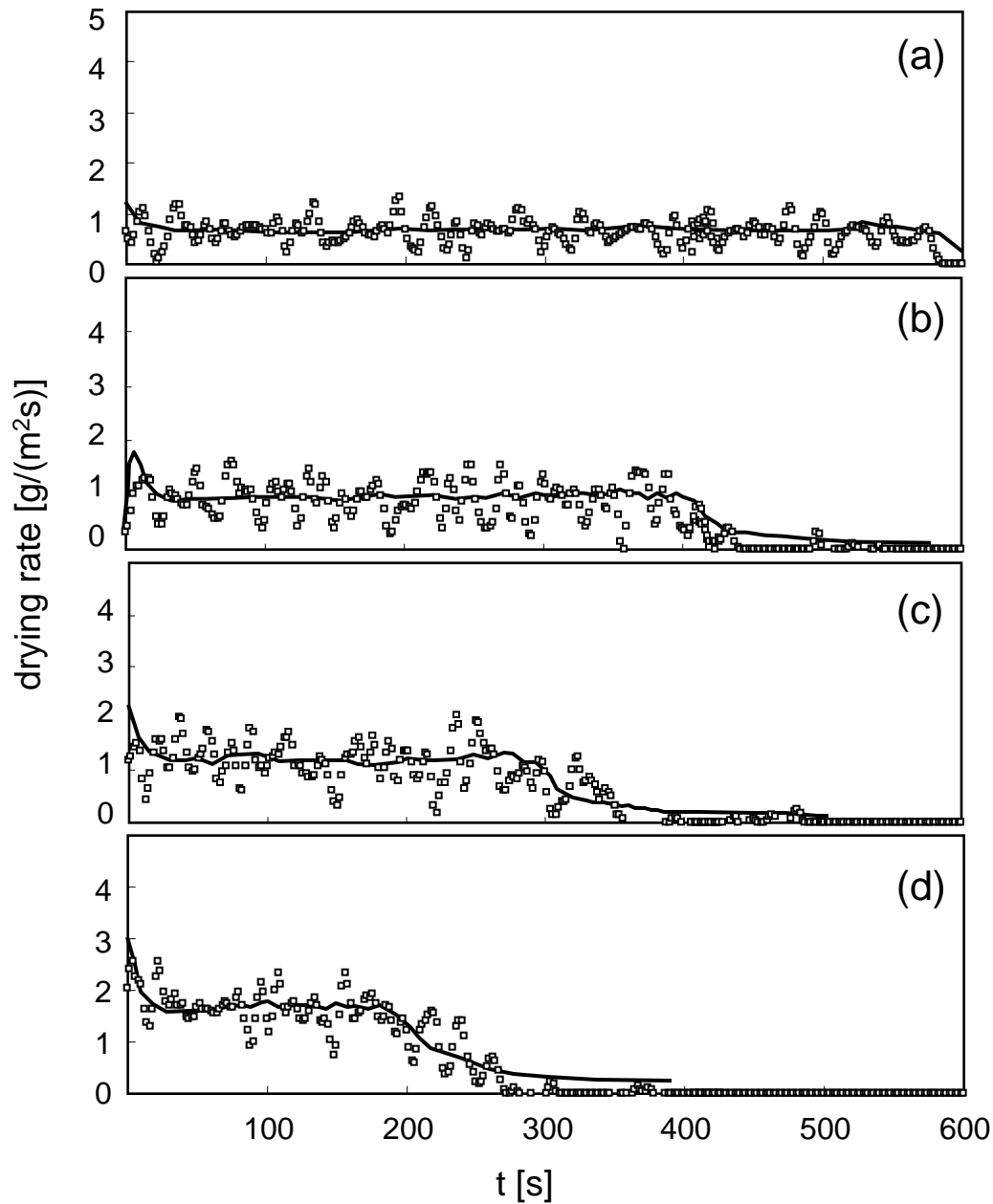


Fig.4 Comparisons between the heat flux (solid curves) and gravimetric (rectangular symbols) methods for four different substrate temperatures of (a)308.2 K, (b)313.2 K, (c)318.2 K and (d) 323.2 K.

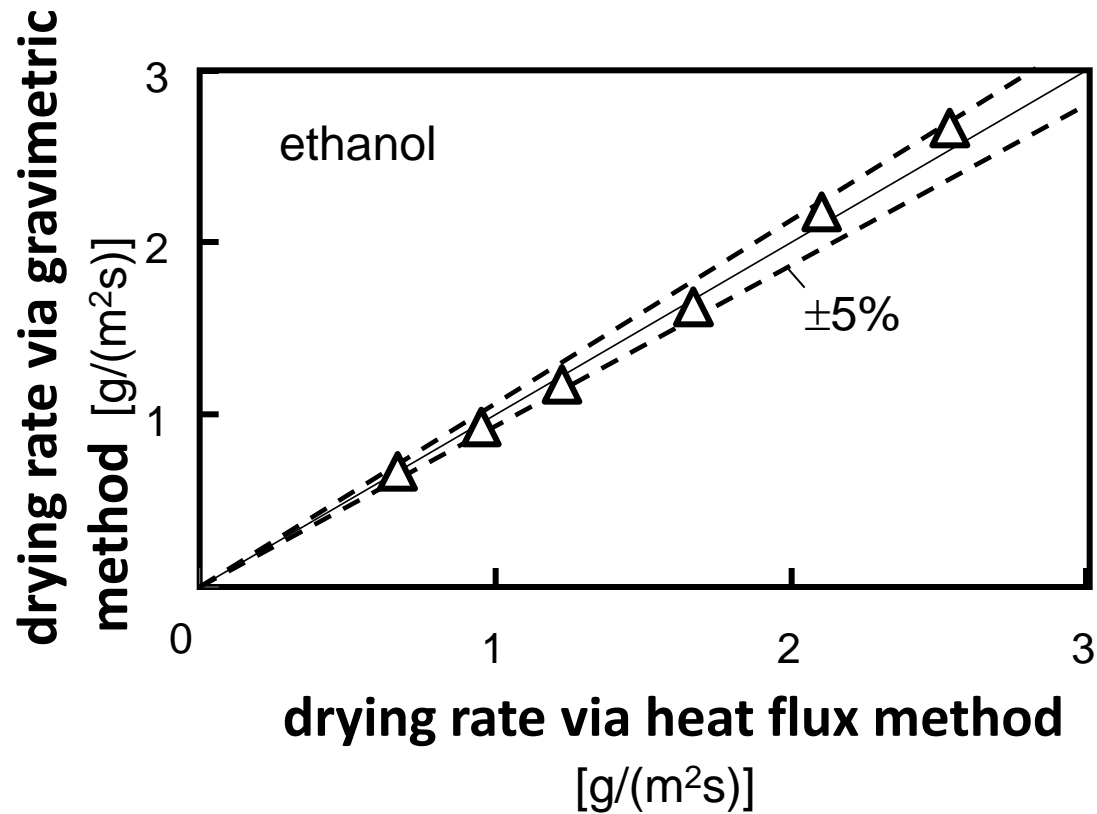


Figure 5 Comparison of the time-averaged drying rates between the heat flux method and the gravimetric method. The measured drying rates agree within a relative error of $\pm 5\%$.